Activation of Nod1 Signaling Induces Fetal Growth Restriction and Death through Fetal and Maternal Vasculopathy

Hirosuke Inoue,* Hisanori Nishio,* Hidetoshi Takada,† Yasunari Sakai,* Etsuro Nanishi,* Masayuki Ochiai,* Mitsuho Onimaru,‡ Si Jing Chen,§ Toshiro Matsui,§ and Toshiro Hara*

Intrauterine fetal growth restriction (IUGR) and death (IUFD) are both serious problems in the perinatal medicine. Fetal vasculopathy is currently considered to account for a pathogenic mechanism of IUGR and IUFD. We previously demonstrated that an innate immune receptor, the nucleotide-binding oligomerization domain-1 (Nod1), contributed to the development of vascular inflammations in mice at postnatal stages. However, little is known about the deleterious effects of activated Nod1 signaling on embryonic growth and development. We report that administration of FK565, one of the Nod1 ligands, to pregnant C57BL/6 mice induced IUGR and IUFD. Mass spectrometry analysis revealed that maternally injected FK565 was distributed to the fetal tissues across placenta. In addition, maternal injection of FK565 induced robust increases in the amounts of CCL2, IL-6, and TNF proteins as well as NO in maternal, placental and fetal tissues. Nod1 was highly expressed in fetal vascular tissues, where significantly higher levels of CCL2 and IL-6 mRNAs were induced with maternal injection of FK565 than those in other tissues. Using *Nod1*-knockout mice, we verified that both maternal and fetal tissues were involved in the development of IUGR and IUFD. Furthermore, FK565 induced upregulation of genes associated with immune response, inflammation, and apoptosis in fetal vascular tissues. Our data thus provided new evidence for the pathogenic role of Nod1 in the development of IUGR and IUFD at the maternal-fetal interface. ***The Journal of Immunology*****, 2016, 196: 2779–2787.**

Intrauterine growth restriction (IUGR), also known as fetal growth restriction, refers to a fetus that has failed to reach his or her genetic growth potential in utero. IUGR is a relatively common, pleiotropic complication of pregnancy, affecting 5–10% of all newborns (1, 2). IUGR is associated with a high incidence of perinatal morbidity and mortality. Neonates born with IUGR have an increased risk of serious neonatal diseases, including neonatal asphyxia, respiratory distress, hypoglycemia, hypocalcemia, and polycythemia (3). In addition, IUGR fetuses have an approximately 5–10-fold increased risk of intrauterine fetal death (IUFD), and it was reported that up to ∼50% of cases of stillbirth or IUFD also involved IUGR (4). Furthermore, epidemiologic evidence has long suggested that newborns with IUGR have an increased risk of cardiovascular disease later in adulthood (2, 5), possibly caused by an endothelial dysfunction related to IUGR. Several conditions, such as maternal factors (e.g., pre-eclampsia, young or advanced age and preconception diet), fetal factors (e.g., genetic causes, congenital malformations, fetal infection), and the placental dysfunction, have been suggested as risk factors for IUGR (2). However, these risk factors are not apparent in 50% of cases (6, 7).

Newborns and fetuses rely heavily on their innate immune system for protection against microorganisms because of the well-described defects in adaptive immunity resulting from limited exposure to Ags in utero (8). Among pattern-recognition receptors (PRRs), TLR 4 has been most intensively studied on its role in maternal-fetal interface or in newborns (9, 10). On the other hand, little is known about the physiologic or pathologic role of other PRRs (e.g., nucleotide binding and oligomerization domain-like receptors [NLRs], integrins, and C-type lectin receptors) in perinatal diseases.

A cytoplasmic PRR, nucleotide-binding oligomerization domain-1 (NOD1) is a member of the NLR family (11, 12). Recently, we demonstrated a specific role of Nod1 in the development of acute vascular inflammation in young mice (13) and atherosclerosis in adult mice (14). On the other hand, the effects of the activation of Nod1 in the fetuses or in newborns have been

*Department of Pediatrics, Graduate School of Medical Sciences, Kyushu University, Fukuoka 812-8582, Japan; †Perinatal and Pediatric Medicine, Graduate School of Medical Sciences, Kyushu University, Fukuoka 812-8582, Japan; ‡Department of Pathophysiological and Experimental Pathology, Graduate School of Medical Sciences, Kyushu University, Fukuoka 812-8582, Japan; and §Department of Bioscience and Bioenvironmental Sciences, Faculty of Agriculture, Graduate School of Kyushu University, Fukuoka 812-8581, Japan

ORCIDs: 0000-0003-3631-7790 (H.N.); 0000-0002-5747-8692 (Y.S.); 0000-0002-1926-2356 (M. Onimaru); 0000-0002-7857-1140 (S.J.C.); 0000-0002-9137-8417 (T.M.).

Received for publication February 9, 2015. Accepted for publication January 5, 2016.

This study was supported in part by the Japan Society for the Promotion of Science (Grants KAKEN 24659509 [to T. Hara] and 15K19656 [to H.I.]), the Morinaga Foundation for Health and Nutrition (to H.I.), the Takeda Science Foundation (to Y.S.) and the Mother and Child Health Foundation (to Y.S.).

The microarray data presented in this article have been submitted to the National Center for Biotechnology Information Gene Expression Omnibus (http://www.ncbi.nlm.nih.gov/geo/) under accession number GSE65188.

Address correspondence and reprint requests to Dr. Hirosuke Inoue, Department of Pediatrics, Graduate School of Medical Sciences, Kyushu University, 3-1-1 Maidashi, Higashi-ku, Fukuoka 812-8582, Japan. E-mail address: hinoue@pediatr.med.kyushu-u.ac.jp

The online version of this article contains supplemental material.

Abbreviations used in this article: E, embryonic day; IUFD, intrauterine fetal death; IUGR, intrauterine growth restriction; LC, liquid chromatography; LC-MS, liquid chromatography–mass spectrometry; LC-MS/MS-MRM, liquid chromatography–tandem mass spectrometry–multiple reaction monitoring; MRM, multiple reaction monitoring; MS, mass spectrometry; NLR, nucleotide binding and oligomerization domain–like receptor; NOD1, nucleotide-binding oligomerization domain-1; PRR, pattern-recognition receptor; TNBS, 2,4,6-trinitrobenzene sulfonate; WT, wild-type.

poorly understood (15–17). In the current study, we found that activation of Nod1 signaling in pregnant mice induced IUGR and IUFD. We also found that maternal and fetal responses against Nod1 ligand (FK565) played an important role in the pathogenesis of IUGR and IUFD. Our observations may lead to the elucidation of a part of the pathogenesis of IUGR, IUFD, and the cardiovascular manifestation in later life in humans.

Materials and Methods

Ligands

The specific Nod1 agonist FK565 (*N*-heptanol $_{L}$-Ala-γ-$_{D}$-Glu-meso-DAP-$_{D}$-Ala, m.w. 502.6 Da) was supplied by Astellas Pharmaceutical (Tokyo, Japan). Synthetic C12-iE-DAP (another ligand for Nod1) was purchased from InvivoGen (San Diego, CA). Toxinometer (ET-5000; Wako Pure Chemical Industries, Osaka, Japan) analysis revealed that endotoxin contamination levels were below the detection limit (0.05 EU/ml) in the FK565 preparation.

Mice

Wild-type (WT) C57BL/6 mice were purchased from KBT Oriental (Charles River Grade; Saga, Japan). Homozygous *Nod1*-knockout (*Nod1*$^{-/-}$) mice in C57BL/6 background were provided by T.W. Mak (University Health Network, Toronto, ON, Canada). Adult female mice (8–12 wk old) were mated, and the day of vaginal plug appearance was designated as embryonic day (E) 0.5. All mice were housed in a specific pathogen-free environment. Experiments were performed under barrier conditions at the animal facility of the biosafety level P1A. All experiments with mice were performed according to the protocol approved by the Kyushu University Institutional Animal Care and Use Committee.

Nod1 genotyping

Tail snips were obtained from mice and used for genotyping. The genotype of the mice was determined by PCR analysis using primers specific to WT and mutant-type Nod1 alleles. Primer pairs for Nod1 WT and mutant-type were 5′-GCTTGGCTCCTTTGTCATTG-3′ and 5′-ACTGCTGCTTGGCTTTATTCTC-3′, and 5′-TTGGTGGTCGAATGGGCAGGTA-3′ and 5′-CGCGCTGTTCTCCTCTTCCTCA-3′, respectively.

In vivo treatment of pregnant mice

Pregnant mice at E14.5 were s.c. injected with either 100 μl PBS or FK565 (1, 10, or 500 μg in 100 μl PBS). Mice were monitored for preterm labor after injection. After the designated period, pregnant mice were sacrificed, and the fetuses and placentae were removed immediately. Sera were collected from pregnant mice and stored at −30°C until analysis. The number of implantation site, the fetal viability, and the weight of fetuses were recorded. Fetal death was identified by the appearance of the fetus, which was significantly small with white discoloration. The organs of the pregnant mice, fetuses, and placentae were fixed in 4% paraformaldehyde and embedded in paraffin. Paraffin sections were stained with H&E and used for pathologic examination. Various tissues were sterilely and immediately isolated from pregnant and fetal mice by using a surgical microscope (Leica M500; Heerbrugg, Switzerland). These maternal tissues at E14.5 and fetal tissues at E18.5 were used for real-time quantitative RT-PCR, organ culture, or microarray analysis.

Organ culture

Various tissues of fetal mice and the placentae at E18.5 were cultured for 24 h in a 96-well plate in DMEM with 10% FBS and 1% penicillin–streptomycin in the presence or absence of an indicated reagent in a CO_2 (5%) incubator at 37°C. Culture supernatants were obtained and stored at −30°C until analysis.

Tissue homogenization and measurement of the protein concentration

Collected fetuses and fetal tissues were homogenized with PBS containing Cell Culture Lysis Reagent (Promega, Madison, WI) and Protease Inhibitor Cocktail (Nacalai Tesque, Kyoto, Japan). The homogenized lysate was centrifuged at 20,000 × *g* for 5 min at 4°C. Protein concentrations of the supernatant were measured by Bio-Rad protein assay (Bio-Rad Laboratories, Hercules, CA). The supernatants were stored at −30°C until analysis. The concentrations of cytokines, NO, and FK565 in the supernatants were expressed as those divided by the tissue protein concentrations of individual samples.

Analysis of cytokines and NO metabolites

The concentrations of IL-6, TNF-α, IL-12p70, IFN-γ, IL-10, and CCL2 were measured by BD Cytometric Bead Array mouse inflammation kit (Becton Dickinson, San Jose, CA) according to the manufacturer's instructions. The concentrations of nitrite were determined using Griess method with the NO_2/NO_3 Assay Kit-C II (Dojin Chemical Laboratory Institute, Kumamoto, Japan).

Detection of FK565

For high-sensitive detection of target FK565 in sera of pregnant mice, and in homogenate supernatants of placentae and fetuses, we applied a liquid chromatography–tandem mass spectrometry–multiple reaction monitoring (LC-MS/MS-MRM) in combination with 2,4,6-trinitrobenzene sulfonate (TNBS) derivatization technique (18). To an aliquot (40 μl) of sample solution, 10 μl of 150 mM TNBS in 0.1 M borate buffer (pH 8.0) was added. After the incubation at 30°C for 60 min, 50 μl of 0.2% formic acid was added to the derivatized mixture, and 10 μl of the mixture was injected into LC-MS. Sample solutions including sera and supernatants used in this study were obtained after filtration with a Millipore Amicon Ultra-0.5 centrifugal filter (m.w. cut of <3000 Da; Millipore, Billerica, MA). The target was detected with an Agilent 1200 HPLC (Agilent Technologies, Waldbronn, Germany) coupled to an Esquire 6000 ESI-Ion Trap mass spectrometer (Bruker Daltonics, Bremen, Germany). A chromatographic separation was performed on a COSMOSIL 5C_{18}-AR-II column (5 μm pore size, 2.0 mm × 150 mm) with a guard column (2.0 × 30 mm; Nacalai Tesque, Kyoto, Japan). A linear gradient elution of 20–100% acetonitrile containing 0.1% FA in 20 min at 0.20 ml/min was performed at 40°C. Electrospray ionization in positive mode was performed as follows: nebulizer gas (N_2), 40 ψ; dry gas (N_2), 8 L/min; dry temperature, 330°C; HV capillary, −2,750 V; HV end plate offset, −500 V; resolution, *m/z* 0.25; target ion trap, 50,000; Oct1, 12.00 V; Oct2, 2.03 V; Trap Drive, 72.7 V. The width for monoisotopic isolation of target precursor ions of TNP-FK565 (*m/z* 714.2 > 625.2) and internal standard (IS; *m/z* 713.2 > 513.2) was set at *m/z* 2.0. These optimized MRM parameters were set individually for TNP-FK565 and TNP-IS via time-segment definitions. For calibration curve, three separate replicates of each of six different concentrations between 0.05 and 50 nmol/L FK565 and 10 μmol/L C12-iE-DAP as an IS were conducted, at which both analytes were spiked with sera to compensate for any MS interference from fluid matrix. The ratio of peak area of FK565 to that of the IS was used for the quantification analysis.

Real-time quantitative RT-PCR

Total RNA was extracted from murine fetal tissues using RNeasy Micro kit or RNeasy Fibrous Tissue Mini kit (Qiagen, Valencia, CA), followed by cDNA synthesis using a First-Strand cDNA Synthesis kit (Amersham Pharmacia Biotech, Piscataway, NJ). The mRNA expression levels of the targeted genes were analyzed with a TaqMan Gene Expression Master Mix and Applied Biosystems StepOnePlus sequence detector (Applied Biosystems, Foster City, CA), as described (19). The primers and probes for the following genes were obtained from Applied Biosystems: *Gapdh* (Mm99999915_g1), *Nod1* (Mm00805062_m1), *Ccl2* (Mm00441242_m1), *Il6* (Mm00446190_m1), *Cxcl16* (Mm00469712_m1), *Ccl8* (Mm01297183_m1), *Ccl5* (Mm01302427_m1). *Gapdh* was used as an internal control.

Microarray analysis

Total RNA was isolated from fetal aorta using TRIzol Reagent (Invitrogen, Carlsbad, CA) and purified using SV Total RNA Isolation System (Promega, Madison, WI). The quality of the RNA was checked using an Experion automated electrophoresis station (Bio-Rad Laboratories, Hercules, CA). The cRNA was amplified and labeled using Low Input Quick Amp Labeling (Agilent Technologies, Santa Clara, CA), and hybridized using SurePrint G3 Mouse Gene Expression Microarray 8 × 60 K (Agilent). All hybridized microarray slides were scanned using an Agilent scanner. Relative hybridization intensities and background hybridization values were calculated using Agilent Feature Extraction Software (version 9.5.1.1). The raw signal intensities of samples were log2-transformed and normalized using the quantile algorithm. To identify upregulated and downregulated genes, the data, from which long intergenic noncoding RNA probes and undetected probes were filtered out, were analyzed using the linear models for microarray data algorithm (20). Next, we calculated ratios (non–log-scaled fold-change) and *p* value statistics, and established criteria for regulated genes: upregulated genes, ratio ≥ 2.0-fold and *p* value < 0.05; downregulated genes, ratio ≤ 0.5 and *p* value < 0.05. To determine significantly overrepresented Gene Ontology (GO) categories and significant enrichment of pathways, we used tools and data provided at the Database for Annotation, Visualization and Integrated Discovery version 6.7 (http://

david.abcc.ncifcrf.gov/home.jsp). A heat map was generated, and hierarchical clustering was done using MeV software (http://www.tm4.org/mev.html). Microarray data were deposited in Gene Expression Omnibus (http://www.ncbi.nlm.nih.gov/geo/) under accession number GSE65188.

Statistical analyses

Statistical analyses were performed with statistical software (JMP; SAS Institute, Cary, NC). Quantitative data were analyzed with the Student *t* test, Dunnett test, or Wilcoxon rank-sum test. Categorical data were analyzed by the χ^2 test or Cochran-Armitage test for trend. Statistical significance was defined as $p < 0.05$.

Results

Nod1 ligand (FK565) induces IUFD and IUGR

To investigate the in vivo effects of Nod1 activation on fetuses, we injected either PBS or low to high doses (1, 10, and 500 μg) of a pure synthetic Nod1 ligand (FK565) to pregnant mice at E14.5. Prior to the following experiments, we found that 13.4% of total embryos showed spontaneous regression of fetal growth with the signs of IUGR and IUFD (Fig. 1A). We thus considered this range of the IUFD rate as physiological backgrounds that were observed in control experiments. At E16.5, the proportion of IUFD increased to 34.1% ($p < 0.0001$) and 78.8% ($p < 0.0001$) of whole embryos with 10 and 500 μg of FK565 treatments, respectively (Fig. 1A). We also found that these effects appeared in a dose-dependent manner (trend $p < 0.0001$; Fig. 1A–C). The proportion (14.8%) of IUFD did not increase at a low dose of FK565 (1 μg; Fig. 1A, 1B). On the other hand, the fetal weight at E16.5 was significantly reduced to 89.1% ($p < 0.0001$) and 83.8% ($p = 0.0001$) of controls with 1- and 500-μg injections of FK565, respectively (Fig. 1D). These data clearly demonstrated that the embryonic growth was affected, even with the low-dose injection of FK565 to the pregnant mice (Fig. 1C, 1D). Notably, a previous report showed that maternal injection of iE-DAP, another Nod1 agonist, induced preterm delivery (21). However, FK565 did not induce preterm delivery at 1 μg (0%, $n = 29$), 10 μg (0%, $n = 11$) or 500 μg (0%, $n = 18$) in our study (Fig. 1E).

Transplacental transfer of FK565 into the fetus

We next investigated whether FK565 injected to pregnant mice transferred to the fetus transplacentally. The detection of FK565 was completed with TNBS derivatization-aided LC-MS/MS-MRM analysis (18). The calibration curve for FK565 showed an acceptable linear correlation (R^2 value > 0.99), and high sensitivity (limit of detection: 0.26 nmol/L; Fig. 2A). As shown in Fig. 2B and 2C, the target FK565 was successfully detected in the sera of pregnant mice as well as in the placental and fetal homogenates 6 h after FK565 administration at a dose of 500 μg. We detected a small peak of FK565 in the fetuses after the administration of 1 μg FK565 to the pregnant mice when we concentrated the samples for the measurement (signal-to-baseline noise ratio of > 10, data not shown). To exclude the possibility that FK565 was delivered to fetal tissues only in the presence of placental inflammation, we

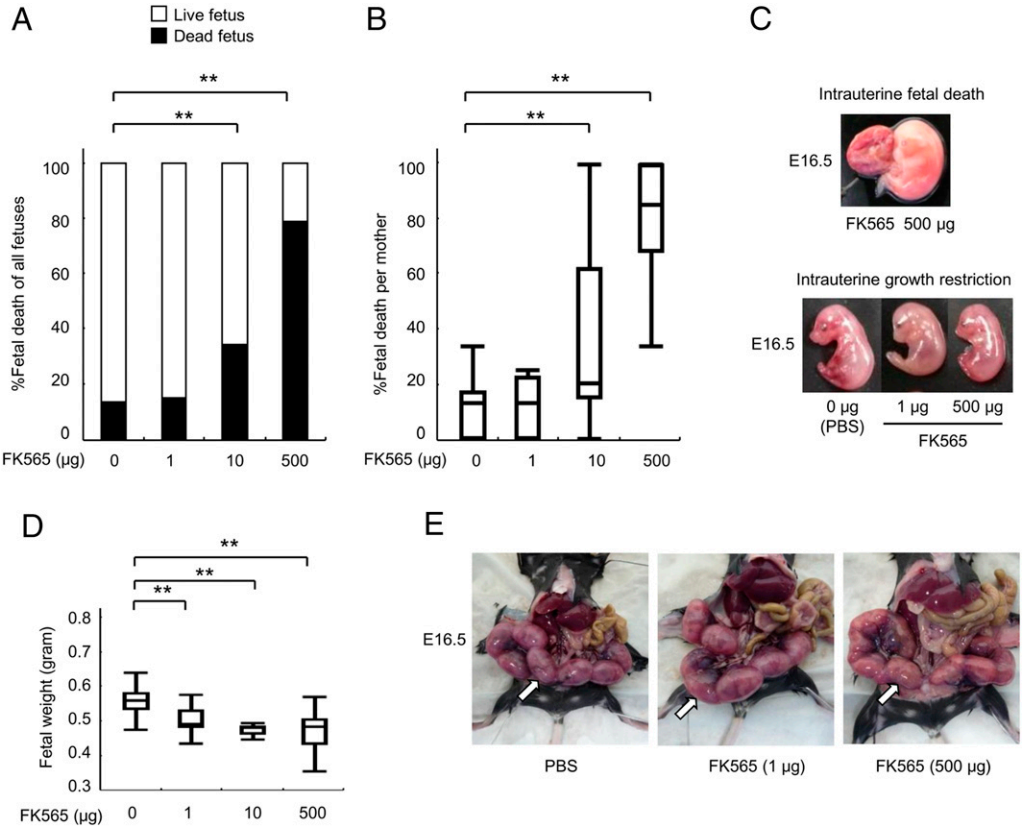

FIGURE 1. Nod1 ligand (FK565) induces IUFD and IUGR. (**A**) Proportion (%) of fetal death after maternal treatment with FK565. The pregnant mice were treated with the indicated dose of FK565 at E14.5. The percentage of the dead fetuses in all fetuses at E16.5 is shown w black bars. (**B**) Proportion (%) of fetal death per mother caused by FK565 treatment. The percentage of the dead fetuses per mother is shown. (**C**) Macroscopic findings of IUFD and IUGR at E16.5. The representative appearances of the fetuses showing IUFD (*top*) and of a fetus showing IUGR (*bottom*) of mothers treated with FK565 are shown. (**D**) Body weight of alive fetuses at E16.5 from pregnant mice that were s.c. treated with the indicated dose of FK565 on E14.5. The mean weight of fetuses per mother is shown. (**E**) Gestational sacs at E16.5 from pregnant mice treated s.c. with FK565 on E14.5. White arrows indicate gestational sacs. Note the absence of preterm delivery, even at high FK565 doses (500 μg). Data are representative of at least 10 pregnant mice. (A, B, and D) Data are shown as the proportions or median with box-and-whiskers plots from 10 or more pregnant mice per group. $^{**}p < 0.01$ relative to the PBS control (Dunnett's test for quantitative data and χ^2 test for categorical data).

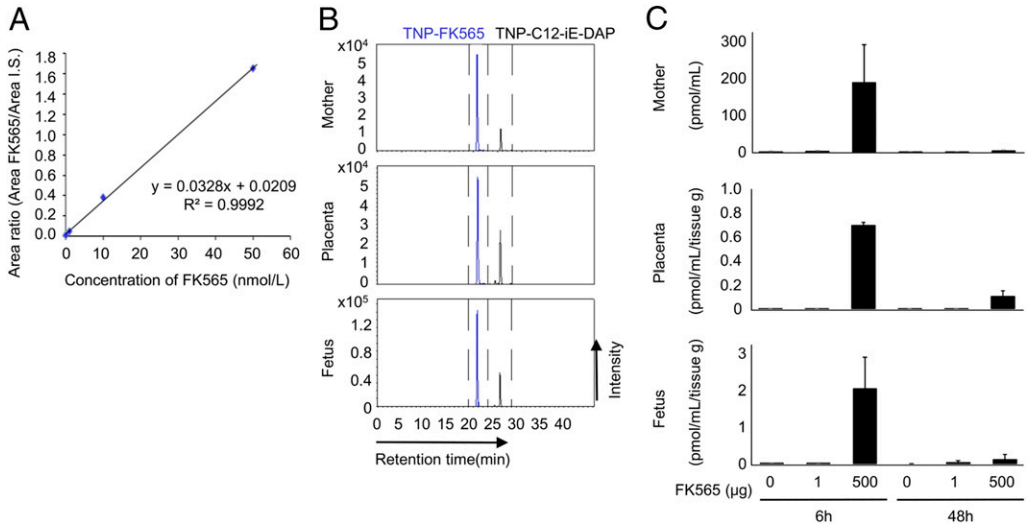

FIGURE 2. The investigation of transplacental transfer of FK565 to a fetus by LC-MS/MS-MRM analysis with TNBS derivatization method. (**A**) A linear calibration curve for FK565 using the TNBS method. FK565 was added to the mouse serum, and the FK565 area was measured by LC-MS/MS-MRM. Experiments were performed three times independently. (**B**) Detection of FK565 in the placenta and fetus 6 h after treatment of the pregnant mice with FK565 at E14.5. C12-iE-DAP was used as the internal control. The results of analysis in serum of a pregnant mouse (*upper panel*), placental homogenate (*middle panel*), and fetal homogenate (*lower panel*) are shown. They are the representative of three independent experiments. (**C**) The levels of FK565 in the serum of the mother, placenta, and fetus. FK565 concentrations in these samples were measured by quantitative analysis based on the calibration curve (n = 3 for each group).

repeated the same experiments using *Nod1*-knockout pregnant mice. FK565 was similarly detected in fetuses after FK565 injection to *Nod1*-knockout pregnant mice (Supplemental Fig. 1A), which indicated that transfer of FK565 was not induced by maternal or placental inflammation.

Inflammatory responses by the administration of FK565 in the pregnant mice, placentae and fetuses

Because inflammatory mediators are induced by Nod1 agonist in vivo and in vitro (22), we analyzed the expression levels of CCL2, IL-6, and TNF-α proteins and the amount of endogenously produced NO in pregnant mice after FK565 treatment. A substantial increase in production of CCL2, IL-6, and NO was observed 6 h after administration of FK565 in the sera of the pregnant mice and placentae at the two different doses (1 and 500 μg; Fig. 3A, 3B); however, CCL2, IL-6, and TNF-α production was induced only at a dose of 500 μg in the fetuses (Fig. 3C). The elevated CCL2, IL-6, TNF-α, and NO levels returned to the control levels within 48 h similarly in the pregnant mice, placentae, and fetuses (Fig. 3A–C).

In this study, we used the same line of *Nod1*-knockout mice that was previously reported (13, 14). FK565 does not induce inflammation in *Nod1*-knockout mice. However, whether the same result can be obtained with pregnant *Nod1*-knockout mice is unknown. No previous studies have examined inflammatory markers in maternal or feto-placental tissues in *Nod1*-knockout mice. Therefore, to examine whether FK565 induces inflammation in pregnant *Nod1*-knockout mice, we injected either PBS or a high dose (500 μg) of FK565 to pregnant *Nod1*-knockout mice at E14.5 (n = 3 for each group). We analyzed the expression levels of CCL2, IL-6, and TNF-α protein in the sera of pregnant mice, placentae, and fetuses 6 h after FK565 treatment. There were only negligible effects on an increase in production of these proteins after treatment (Supplemental Fig. 1B). Moreover, FK565 was detected in the placenta and fetus after FK565 injection to these mice (Supplemental Fig. 1A). Therefore, we conclude that FK565 does not induce inflammation in maternal and feto-placental tissues in pregnant *Nod1*-knockout mice.

We previously found that the administration of FK565 induced vascular inflammation in young mice (5–9 wk old) (13) and atherosclerosis in adult mice (14). Therefore, we examined whether FK565 induced vascular inflammation in fetal mice. However, no inflammatory cells were observed around the coronary arteries of the pregnant mice, placentae, and live fetuses in this condition (Fig. 3D). A high dose of FK565 induced vascular inflammation in pregnant mice, but not in placentae or fetuses (Supplemental Fig. 2). Pathologic necrosis, hemorrhage, or edema was not apparent in any tissue of FK565-treated pregnant mice, placentae, and live fetuses (data not shown).

Fetal vascular tissue is a major site of action of Nod1 ligand (FK565)

We investigated the physiologic expression levels of Nod1 in various fetal tissues, including the placenta and yolk sac, at E18.5 by real-time quantitative PCR. Nod1 mRNA expression was ubiquitous and detected in all fetal tissues examined. Among them, a high Nod1 mRNA expression was observed in vascular tissues, lung, and spleen (Fig. 4A). As previously described, Nod1 mRNA was expressed weakly in the fetal heart (16).

Based on these results, we tested whether the fetal tissues could respond to Nod1 ligand. Various tissues of fetal mice, including the placenta and yolk sac, were dissected from pregnant mice at E18.5. The production of CCL2 and IL-6 was investigated with ex vivo organ culture of each fetal tissue in the presence or absence of FK565. A significant amount of CCL2 and IL-6 was released only from the vascular tissues (aortic arch and aortic artery) in response to FK565 (Fig. 4B). To validate these findings in vivo, various tissues of fetal mice, including the placenta and yolk sac, were separated from E18.5 pregnant mice 6 h after injection of FK565, and mRNA expression levels in these tissues were determined with real-time quantitative PCR. Consistent with data from the ex vivo organ culture, upregulation of CCL2 and IL-6 mRNAs was most apparent in the vascular tissues of fetus (“aortic arch” and “aortic artery”; Fig. 4C). Similarly, CCL2 and IL-6 mRNAs were also upregulated in the vascular tissues of the pregnant mice at E14.5 at 6 h after injection of FK565 (Fig. 4D).

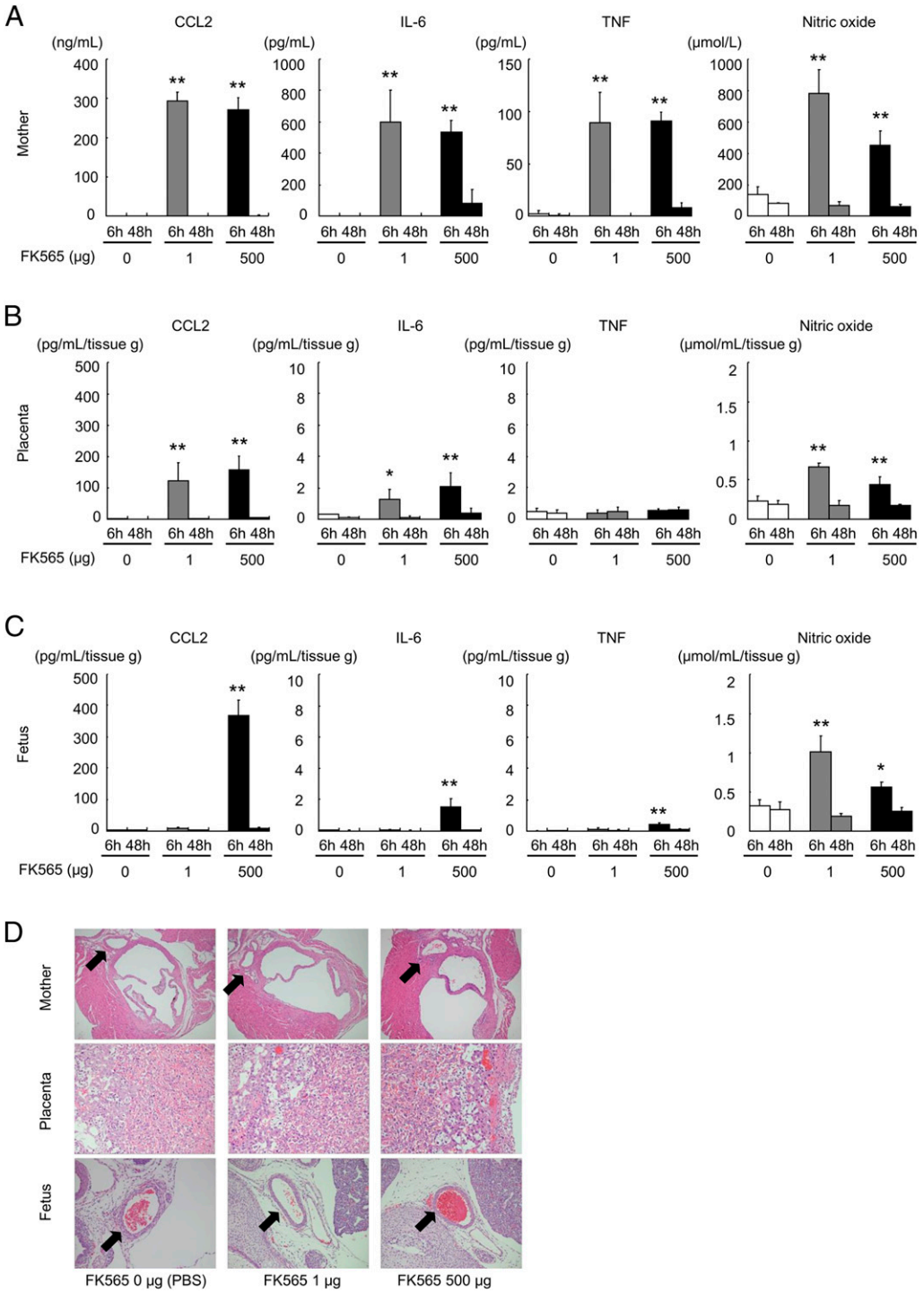

FIGURE 3. Effect of FK565 on the production of CCL2, IL-6, TNF, and NO in sera from pregnant mice, placentae, and fetuses. (**A**–**C**) Cytokine, chemokine, and NO levels were determined in the samples [(A), serum of the mother; (B), placental homogenates; (C), fetal homogenates] after 6 and 48 h from pregnant mice treated with indicated doses of FK565 at E14.5. The mean values and standard deviations are shown (n = 4–5 for each group). (**D**) Histologic evaluation of pregnant mice, placentae, and live fetuses. The perivascular regions are indicated with arrows. *$p < 0.05$; **$p < 0.01$ relative to the PBS (0 μg of FK565) 6-h control (Dunnett test).

Nod1 ligand (FK565) has direct effects on fetal vascular system

We then determined the pathogenic effects of transplacentally transferred FK565 on fetuses. The proportion of IUFD was assessed with various combinations of parental *Nod1* genotypes. As mentioned above (Fig. 1A), significantly higher proportion (78.8%) of IUFD was observed with the injection of FK565 (500 μg) to the WT pregnant mice, and weaker effects on embryos were obtained when the paternal genotype was $Nod1^{-/-}$ (65.1% of IUFD, Fig. 5A). By contrast, when FK565 was injected to $Nod1^{-/-}$ pregnant mice, IUFD (13.9%) was never induced (Fig. 5A). Of note, a significantly lower proportion (7.1%) of IUFD was obtained in $Nod1^{-/-}$ fetuses than those in $Nod1^{-/+}$ fetuses (41.9%) when $Nod1^{-/+}$ pregnant mice were injected with

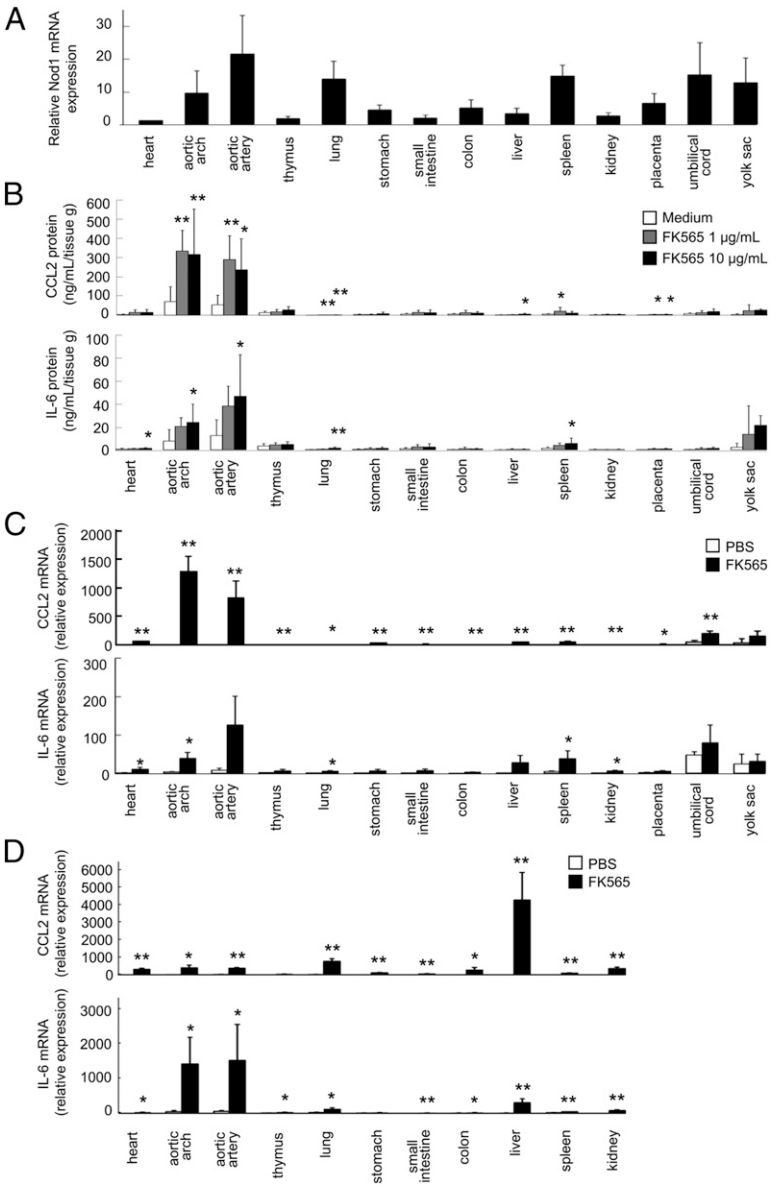

FIGURE 4. Nod1 expression and cytokine production in responses to Nod1 ligand (FK565) stimulation in various tissues of the fetus. (**A**) Nod1 expression levels in various tissues of normal fetal mice at E18.5. The mRNA expression levels were determined by real-time quantitative PCR with *Gapdh* as the internal control. The relative Nod1 mRNA expression levels in each tissue were determined relative to the mRNA level in heart (set as 1.0). The bar indicates mean and SD ($n = 3$). (**B**) The production of cytokines in various tissues of normal fetal mice at E18.5 ex vivo treated with FK565. Each bar indicates mean and SD ($n = 8$ for each group). $*p < 0.05$, $**p < 0.01$ relative to medium (Dunnett test). (**C**) The expression of cytokines in various tissues of fetal mice from pregnant mice treated with FK565 at a dose of 500 μg on E18.5. The relative mRNA expression levels in each tissue were determined relative to the mRNA level in heart treated with PBS (1.00). Each bar indicates mean and SD ($n = 3$ for each group). $*p < 0.05$, $**p < 0.01$ relative to each tissue treated with PBS (Student t test). (**D**) The expression of cytokines in various tissues of pregnant mice treated with FK565 at a dose of 500 μg on E14.5. The relative mRNA expression levels in each tissue were determined relative to the mRNA level in heart treated with PBS (1.00). Each bar indicates mean and SD ($n = 3$ for each group). $*p < 0.05$, $**p < 0.01$ relative to each tissue treated with PBS (Student t test).

FK565 ($p = 0.0007$, Fig. 5A). However, fetal weight was significantly reduced in WT and *Nod1* $^{-/+}$ pregnant mice with 500-μg injections of FK565 compared with controls (Fig. 5B). There was no significant difference in fetal weight between the genotypes of the fetuses (*Nod1*$^{+/+}$ versus *Nod1*$^{-/+}$ or *Nod1*$^{-/+}$ versus *Nod1*$^{-/-}$) from pregnant mice of the same genotype (*Nod1*$^{+/+}$ or *Nod1*$^{-/+}$). These findings clearly demonstrated that IUFD and IUGR with FK565 injection resulted from the maternal and fetal reactions to the activated signaling downstream to Nod1.

To identify which tissues might mediate the unfavorable effects of FK565 on fetal growth, we first mated *Nod1*$^{-/-}$ female mice with *Nod1*$^{-/+}$ males. Pregnant mice were s.c. injected with 500 μg FK565 at E18.5. Six hours later, fetoplacental tissues (fetal heart, aortic artery, placenta, and yolk sac) were dissected from pregnant mice, and mRNA expression in these tissues was determined by real-time quantitative PCR. We found that the aortic artery from *Nod1* $^{-/+}$ fetus expressed CCL2 and IL-6 mRNA at the highest level among the tissues that were studied ($n = 3$ for each group; $p < 0.01$). The high expression levels of CCL2 and IL-6 mRNA were not observed with the aortic artery from *Nod1*$^{-/-}$ fetuses (Supplemental Fig. 3).

Because FK565 predominantly induced a vascular response in the fetus (Fig. 4B, 4C; Supplemental Fig. 3), transcriptomic analysis was performed to examine the molecular mechanisms of IUFD after the treatment of pregnant mice with FK565. Microarray analysis was performed on aortic arteries from *Nod1*$^{-/+}$ and *Nod1*$^{-/-}$ littermate fetuses. A total of 1938 out of 39,430 probe sets were considered to be differentially expressed in *Nod1*$^{-/+}$ and *Nod1*$^{-/-}$ fetuses (1028 upregulated and 910 downregulated) when 2-fold expression changes were set at the cutoff limits (Fig. 6A, Supplemental Table I). The accuracy of the microarray data were evaluated through a validation study using real-time PCR assays of five randomly selected genes (Fig. 6B), indicating that high-quality data were reproducibly yielded from the microarray analysis.

To identify specific molecular pathways associated with the FK565-induced IUGR and IUFD, we further performed gene ontology (GO) analyses on the microarray data (Fig. 6C). The majority of top 20 GO categories were associated with the processes of "immune system," "inflammation," and "apoptosis." To verify these data, we submitted the microarray data to Kyoto Encyclopedia of Genes and Genomes (KEGG) pathway database (http://www.genome.jp/kegg/). The KEGG analysis showed that

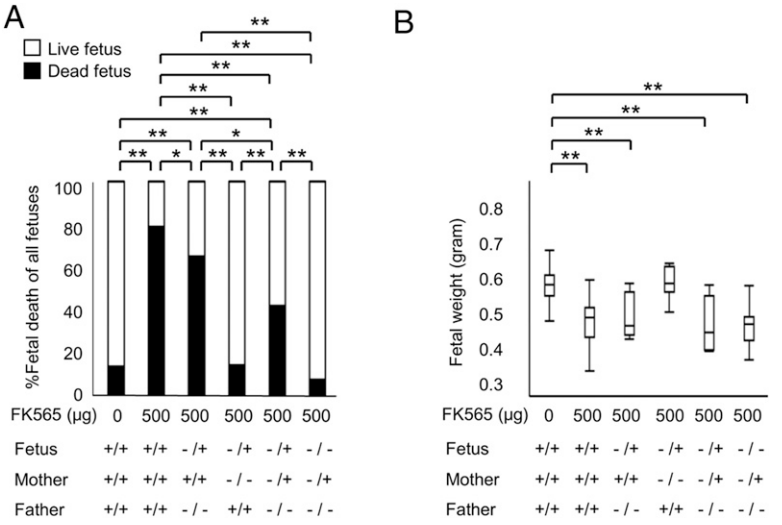

FIGURE 5. Fetal outcome as a direct consequence of maternally administered FK565. (**A**) Proportion (%) of the fetal death at E16.5 from the pregnant mice treated s.c. with FK565 on E14.5 with the combination of indicated Nod1 genotype of parents. Data are shown as the proportion from 7 or more pregnant mice per group. $*p < 0.05$, $**p < 0.01$, χ^2 test. (**B**) Body weight of fetuses at E16.5 from pregnant mice that were treated s.c. with FK565 on E14.5 with the combination of indicated Nod1 genotypes of the parents. The mean weight of fetuses per mother is shown. Data are shown as the median with box-and-whiskers plots from seven or more pregnant mice per group. $**p < 0.01$ (Student t test).

molecular pathways associated with both inflammatory responses and apoptosis were significantly enriched in the aberrantly expressed gene group (Fig. 6D). In line with the GO analysis, "cytokine-cytokine receptor interaction," "NOD-like receptor signaling." "chemokine signaling," "cell adhesion molecules," and "apoptosis" were annotated at the top 20 of the KEGG analysis. Together, the GO and KEGG analyses confirmed the specificity in molecular events and the pathogenic relevance of activated Nod1 signaling to the IUGR and IUFD in this study.

Collectively, our data provided biological evidence that inflammatory responses in fetal vascular tissues were induced by the maternal injection of Nod1 ligand FK565, thereby contributing to the development of IUFD.

Discussion

To our knowledge, this study first demonstrated in vivo evidence that inflammatory responses in pregnant mice upon activated Nod1 signaling severely affected their fetal growth and survival. The present study also clarified that Nod1-associated inflammatory responses in both maternal and fetal vascular tissues contributed to the pathogeneses of IUGR and IUFD that were mimicked by maternal injection of FK565.

Nod1 is a member of the NLR family that is ubiquitously expressed in various tissues. Nod1 detects dipeptide γ-$_D$-Glu-meso-diaminopimelic acid (iE-DAP), which is present in the peptidoglycan of most Gram-negative bacteria such as *Escherichia coli* and certain Gram-positive bacteria (11, 12, 23). DAP-containing bacteria release Nod1 ligands into the environment, and Nod1 ligands are stable in higher temperatures or under acidic or basic conditions (23). It has been suggested that the chronic stimulation of the host immune system by various bacteria present in the environment and food may be associated with the development of allergic diseases in some circumstances (11). In addition, there is a line of evidence that bacterial cell wall components produced by the gut microbiota might translocate out of the lumen of the gut. Karakawa et al. (24) suggested that $_D$-Ala, one of the components of bacterial peptidoglycan in the rat tissues and physiological fluids, was mostly derived from intestinal bacteria. Clarke et al. (25) reported that gut microbiota–derived Nod1 ligands were detected in serum of mice and served as a molecular mediator responsible for the systemic priming of innate immunity. These findings suggest that microbial ligands of PRRs including Nod1 from normal or pathological microbiota might circulate through the body at sufficient concentrations to influence cellular function. Our study showed that Nod1 ligands in pregnant mice could transfer to the fetuses, and the fetuses might be affected directly by Nod1 ligands depending on the Nod1 genotype of the fetus (Fig. 5A). These results suggest that activated Nod1 signaling in the fetus has an important role in the pathogenesis of IUGR or IUFD.

A recent study demonstrated that administration of iE-DAP to pregnant mice caused preterm birth, reduced fetal weight, and induced proinflammatory responses at the maternal-fetal interface (21), which was in part consistent with our study. We found new evidence that among the various fetal tissues, including the placenta and yolk sac, the production of CCL2 and IL-6 after the stimulation with FK565 was observed predominantly in the vascular tissue, wherein Nod1 was expressed at high levels in a physiological condition. We have recently reported that Nod1 signaling was involved in the pathogenesis of the vascular inflammation (13) and arteriosclerosis (14). Other groups also reported that stimulation of Nod1 directly activated blood vessels and induced the inflammatory response via activation of NF-κB and MAPK pathways, which eventually caused experimental shock in vivo (26, 27). However, there was no evidence of cellular infiltration in the arteries of the placentae or fetuses in the current study, which is similar to a previous study using another Nod1 ligand (iE-DAP) (21). When a higher dose of FK565 was injected into pregnant mice, vascular inflammation was induced only in the pregnant mice, but not in the fetal and maternal vessels of the placentae or fetuses (Supplemental Fig. 2). These data might be explained by the effects of pregnancy and by immaturity of fetal immune and vascular systems. Although the site-specific nature of vascular inflammation in response to Nod1 agonist is not completely understood, these results indicate that vascular tissue could be a major site of action of Nod1-related inflammation in fetuses, neonates, and adults.

Earlier reports have shown that the risk of cardiovascular diseases in human adults was higher among those with IUGR (28) (29). The underlying mechanism that mediates the association between the perturbed fetal condition and the development of cardiovascular disease in later life has been incompletely understood. Human clinical and in vitro studies showed that the aortic intima–media layers of IUGR fetuses and neonates were thicker than those of fetuses and neonates with normal growth (5), and the endothelial progenitor cells of IUGR infants had impaired angiogenic properties and tubular formation (30). These observa-

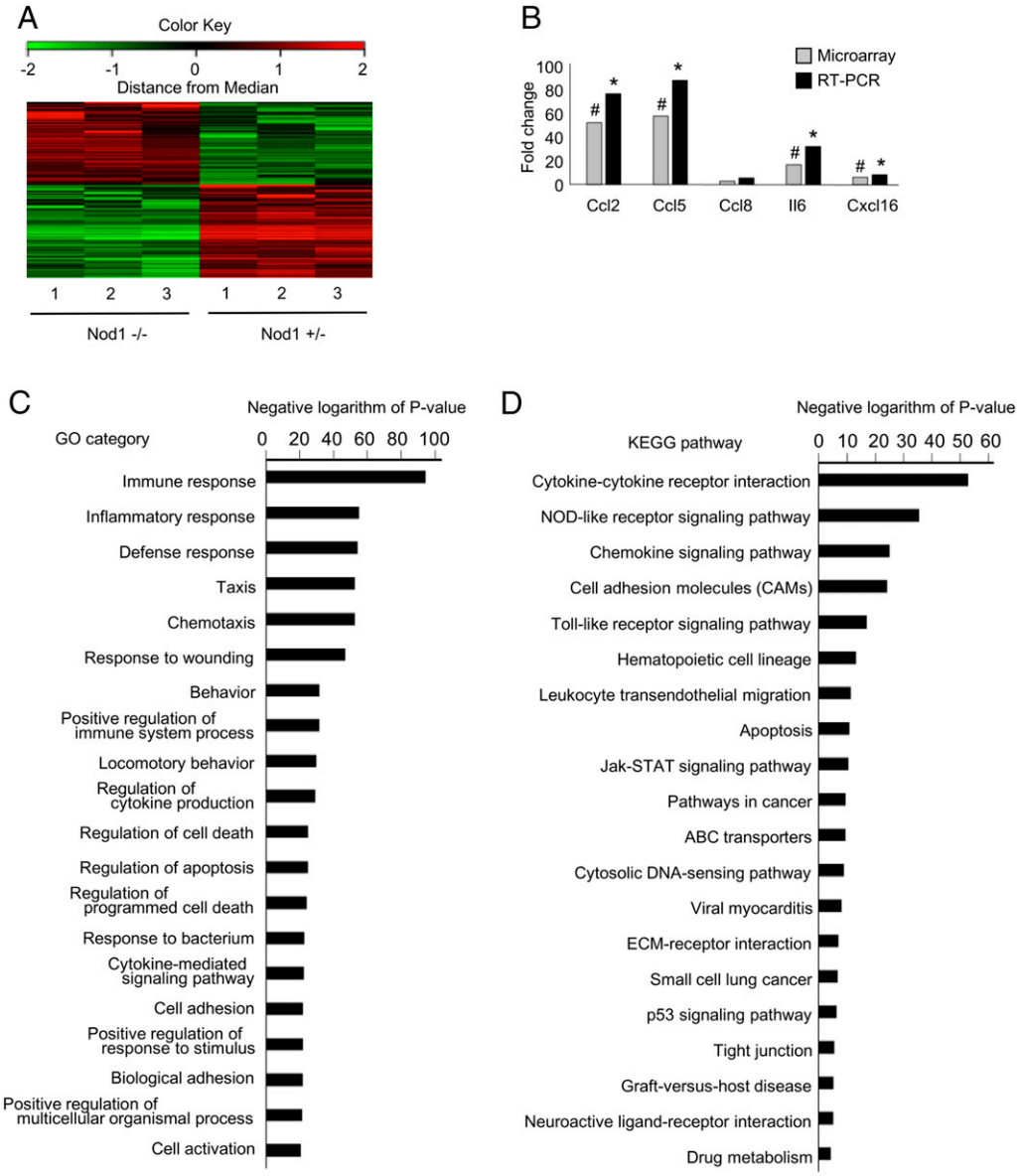

FIGURE 6. Gene expression profiles of vascular tissues from Nod1-heterozygous and knockout fetuses. (**A**) Gene expression profiles of vascular tissues from *Nod1*-heterozygous (*Nod1* $^{-/+}$) and knockout (*Nod1* $^{-/-}$) fetuses are shown. A summary of clustering analysis is graphically shown as a heat map. At the top of this panel, a color key denotes the gradient scale of gene expression from low (green) to high (red) degrees. Each color pixel represents the probed gene on the microarray. The annotated numbers at the bottom indicate the origin of the sample (heterozygous or knockout fetuses). (**B**) Validation of cDNA microarray by quantitative RT-PCR. The bar represents the mean value of each group ($n = 3$ for each group). Annotated bars with symbols ($^{\#}$ and *) indicate the genes that were significantly upregulated in the *Nod1* $^{-/+}$ group by microarray analysis (linear models for microarray data–adjusted $p < 0.05$) and RT-PCR (Student t test $p < 0.05$), respectively. (**C** and **D**) Summary of GO and KEGG pathway analyses for differentially expressed genes in the aorta from *Nod1*-heterozygous and knockout fetuses ($n = 3$ for each group). Functional categories of gene ontology and KEGG databases are listed on the *left*. The bar plots show the values of the negative logarithm of the p value for enrichment of each category group. The larger the size of the bar, the smaller the p value for enrichment of each category.

tions have suggested that the vascular systems of IUGR patients were impaired. This study found that the Nod1 signaling pathway in fetuses contributed to vascular responses and IUGR. Further study is required to determine whether stressful conditions in utero could be a risk for vasculopathy in young (13) and adult mice (14). Further study is required to examine whether Nod1 ligand-induced vasculopathy during fetal life would lead to an increased susceptibility to cardiovascular diseases in adulthood.

In conclusion, our study provides new insight into the association between Nod1 signaling in fetus and the pathophysiology of IUGR and IUFD. These findings offer a framework for unraveling the molecular mechanisms of fetal pathological conditions and adult vascular disease from the standpoint of maternal and fetal environment.

Acknowledgments

We thank Tamami Tanaka and Ayumi Tahara (Department of Pediatrics, Graduate School of Medical Sciences, Kyushu University) for technical support, Chiwa Aikawa (Department of Bioscience and Bioenvironmental Sciences, Faculty of Agriculture, Graduate School of Kyushu University) for the LC-MS/MS-MRM analysis, and Kaori Yasuda (Cell Innovator) for the microarray gene expression analysis.

Disclosures

The authors have no financial conflicts of interest.

References

1. Frøen, J. F., J. O. Gardosi, A. Thurmann, A. Francis, and B. Stray-Pedersen. 2004. Restricted fetal growth in sudden intrauterine unexplained death. *Acta Obstet. Gynecol. Scand.* 83: 801–807.
2. Suhag, A., and V. Berghella. 2013. Intrauterine growth restriction (IUGR): etiology and diagnosis. *Curr. Obstet. Gynecol. Rep.* 2: 102–111.
3. Halliday, H. L. 2009. Neonatal management and long-term sequelae. *Best Pract. Res. Clin. Obstet. Gynaecol.* 23: 871–880.
4. Gardosi, J., S. M. Kady, P. McGeown, A. Francis, and A. Tonks. 2005. Classification of stillbirth by relevant condition at death (ReCoDe): population based cohort study. *BMJ* 331: 1113–1117.
5. Cosmi, E., T. Fanelli, S. Visentin, D. Trevisanuto, and V. Zanardo. 2011. Consequences in infants that were intrauterine growth restricted. *J. Pregnancy.* DOI: 10.1155/2011/364381.
6. McCowan, L. M., C. T. Roberts, G. A. Dekker, R. S. Taylor, E. H. Chan, L. C. Kenny, P. N. Baker, R. Moss-Morris, L. C. Chappell, and R. A. North, SCOPE Consortium. 2010. Risk factors for small-for-gestational-age infants by customised birthweight centiles: data from an international prospective cohort study. *BJOG* 117: 1599–1607.
7. Sato, Y., K. Benirschke, K. Marutsuka, Y. Yano, K. Hatakeyama, T. Iwakiri, N. Yamada, Y. Kodama, H. Sameshima, T. Ikenoue, and Y. Asada. 2013. Associations of intrauterine growth restriction with placental pathological factors, maternal factors and fetal factors; clinicopathological findings of 257 Japanese cases. *Histol. Histopathol.* 28: 127–132.
8. Levy, O. 2007. Innate immunity of the newborn: basic mechanisms and clinical correlates. *Nat. Rev. Immunol.* 7: 379–390.
9. Koga, K., and G. Mor. 2010. Toll-like receptors at the maternal-fetal interface in normal pregnancy and pregnancy disorders. *Am. J. Reprod. Immunol.* 63: 587–600.
10. Kollmann, T. R., O. Levy, R. R. Montgomery, and S. Goriely. 2012. Innate immune function by Toll-like receptors: distinct responses in newborns and the elderly. *Immunity* 37: 771–783.
11. Philpott, D. J., M. T. Sorbara, S. J. Robertson, K. Croitoru, and S. E. Girardin. 2014. NOD proteins: regulators of inflammation in health and disease. *Nat. Rev. Immunol.* 14: 9–23.
12. Caruso, R., N. Warner, N. Inohara, and G. Núñez. 2014. NOD1 and NOD2: signaling, host defense, and inflammatory disease. *Immunity* 41: 898–908.
13. Nishio, H., S. Kanno, S. Onoyama, K. Ikeda, T. Tanaka, K. Kusuhara, Y. Fujimoto, K. Fukase, K. Sueishi, and T. Hara. 2011. Nod1 ligands induce site-specific vascular inflammation. *Arterioscler. Thromb. Vasc. Biol.* 31: 1093–1099.
14. Kanno, S., H. Nishio, T. Tanaka, Y. Motomura, K. Murata, K. Ihara, M. Onimaru, S. Yamasaki, H. Kono, K. Sueishi, and T. Hara. 2015. Activation of an innate immune receptor, Nod1, accelerates atherogenesis in Apoe$^{-/-}$ mice. *J. Immunol.* 194: 773–780.
15. Enoksson, M., K. F. Ejendal, S. McAlpine, G. Nilsson, and C. Lunderius-Andersson. 2011. Human cord blood-derived mast cells are activated by the Nod1 agonist M-TriDAP to release pro-inflammatory cytokines and chemokines. *J. Innate Immun.* 3: 142–149.
16. Inohara, N., T. Koseki, L. del Peso, Y. Hu, C. Yee, S. Chen, R. Carrio, J. Merino, D. Liu, J. Ni, and G. Núñez. 1999. Nod1, an Apaf-1-like activator of caspase-9 and nuclear factor-kappaB. *J. Biol. Chem.* 274: 14560–14567.
17. Granland, C., T. Strunk, J. Hibbert, A. Prosser, K. Simmer, D. Burgner, P. Richmond, and A. J. Currie. 2014. NOD1 and NOD2 expression and function in very preterm infant mononuclear cells. *Acta Paediatr.* 103: e212–e218.
18. Hashimoto, C., Y. Iwaihara, S. J. Chen, M. Tanaka, T. Watanabe, and T. Matsui. 2013. Highly-sensitive detection of free advanced glycation end-products by liquid chromatography-electrospray ionization-tandem mass spectrometry with 2,4,6-trinitrobenzene sulfonate derivatization. *Anal. Chem.* 85: 4289–4295.
19. Ikeda, K., K. Yamaguchi, T. Tanaka, Y. Mizuno, A. Hijikata, O. Ohara, H. Takada, K. Kusuhara, and T. Hara. 2010. Unique activation status of peripheral blood mononuclear cells at acute phase of Kawasaki disease. *Clin. Exp. Immunol.* 160: 246–255.
20. Smyth, G. K. 2004. Linear models and empirical bayes methods for assessing differential expression in microarray experiments. *Stat. Applications. Genet. Mol. Biol.* 3: 1–25.
21. Cardenas, I., M. J. Mulla, K. Myrtolli, A. K. Sfakianaki, E. R. Norwitz, S. Tadesse, S. Guller, and V. M. Abrahams. 2011. Nod1 activation by bacterial iE-DAP induces maternal-fetal inflammation and preterm labor. *J. Immunol.* 187: 980–986.
22. Fritz, J. H., L. Le Bourhis, G. Sellge, J. G. Magalhaes, H. Fsihi, T. A. Kufer, C. Collins, J. Viala, R. L. Ferrero, S. E. Girardin, and D. J. Philpott. 2007. Nod1-mediated innate immune recognition of peptidoglycan contributes to the onset of adaptive immunity. *Immunity* 26: 445–459.
23. Hasegawa, M., K. Yang, M. Hashimoto, J. H. Park, Y. G. Kim, Y. Fujimoto, G. Nuñez, K. Fukase, and N. Inohara. 2006. Differential release and distribution of Nod1 and Nod2 immunostimulatory molecules among bacterial species and environments. *J. Biol. Chem.* 281: 29054–29063.
24. Karakawa, S., Y. Miyoshi, R. Konno, S. Koyanagi, M. Mita, S. Ohdo, and K. Hamase. 2013. Two-dimensional high-performance liquid chromatographic determination of day-night variation of D-alanine in mammals and factors controlling the circadian changes. *Anal. Bioanal. Chem.* 405: 8083–8091.
25. Clarke, T. B., K. M. Davis, E. S. Lysenko, A. Y. Zhou, Y. Yu, and J. N. Weiser. 2010. Recognition of peptidoglycan from the microbiota by Nod1 enhances systemic innate immunity. *Nat. Med.* 16: 228–231.
26. Moreno, L., S. K. McMaster, T. Gatheral, L. K. Bailey, L. S. Harrington, N. Cartwright, P. C. Armstrong, T. D. Warner, M. Paul-Clark, and J. A. Mitchell. 2010. Nucleotide oligomerization domain 1 is a dominant pathway for NOS2 induction in vascular smooth muscle cells: comparison with Toll-like receptor 4 responses in macrophages. *Br. J. Pharmacol.* 160: 1997–2007.
27. Cartwright, N., O. Murch, S. K. McMaster, M. J. Paul-Clark, D. A. van Heel, B. Ryffel, V. F. Quesniaux, T. W. Evans, C. Thiemermann, and J. A. Mitchell. 2007. Selective NOD1 agonists cause shock and organ injury/dysfunction in vivo. *Am. J. Respir. Crit. Care Med.* 175: 595–603.
28. Barker, D. J., P. D. Winter, C. Osmond, B. Margetts, and S. J. Simmonds. 1989. Weight in infancy and death from ischaemic heart disease. *Lancet* 2: 577–580.
29. Gluckman, P. D., and M. A. Hanson. 2004. Living with the past: evolution, development, and patterns of disease. *Science* 305: 1733–1736.
30. Ligi, I., S. Simoncini, E. Tellier, P. F. Vassallo, F. Sabatier, B. Guillet, E. Lamy, G. Sarlon, C. Quemener, A. Bikfalvi, et al. 2011. A switch toward angiostatic gene expression impairs the angiogenic properties of endothelial progenitor cells in low birth weight preterm infants. *Blood* 118: 1699–1709.